URSI GASS 2023, Sapporo, Japan, 19 – 26 August 2023

The Optical Design of the Canadian Galactic Emission Mapper Radio Telescope: Minimizing Polarization Systematics with an Optimized Hat Feed Design

Joshua W. MacEachern*[(1)]
(1) University of British Columbia, Vancouver, Canada; e-mail: maceachern@phas.ubc.ca

Abstract

We describe the optical design to date for the Canadian Galactic Emission Mapper radio telescope, which will conduct an 8-10 GHz Northern sky polarization survey. The optical design is a hat feed, ring focus design that exhibits high polarization purity. We present an optimization framework that can directly minimize our most important polarization systematic, which is the leakage of intensity to polarized intensity ($T \to P$ leakage), in addition to other measures of the instrumental performance. Compared to the initial design, the optimized design exhibits higher forward gain, $T \to P$ leakage that is reduced by several orders of magnitude, and the return loss is better than -20 dB over most of the band.

1 Introduction

The Canadian Galactic Emission Mapper (CGEM) radio telescope will conduct a Northern sky polarization survey between 8 and 10 GHz to aid in the search for a signature of primordial gravitational waves (PGWs) in the polarization of the Cosmic Microwave Background (CMB). If detected, this signature would allow us to probe some of the highest energy physics in the known universe [1]. Unfortunately, the PGW signature is constrained to be extremely faint and are dominated in brightness by polarized foreground emission from our own galaxy that lies between us and the CMB [1]. It is therefore essential to map polarized foreground emission in detail in order for foreground emission to be accurately modelled in CMB data [1]. CGEM will make precise large-area polarization maps of synchrotron emission, an important polarized foreground component, and these maps will be used to improve foreground models to aid in the search for the PGW signature. CGEM must make high-sensitivity polarization measurements with minimal systematics in order to be an aid to CMB experiments, and this principle is central to every design decision that we make as we design the experiment. Accordingly, we have chosen to use a Gregorian, ring-focus, "hat feed" [2], optical design for CGEM. This design inherently offers unparalleled polarization purity, and we've further optimized the polarization purity of the design. In this paper, we describe the design process to date of our hat feed design and showcase the simulated performance of the design. In Section 2, we describe the starting point hat feed system. In Section 3, we describe our optical design optimization procedure. In Section 4, we compare the simulated performance of the starting point design with the performance of the optimized design. We give concluding remarks in Section 5. We note that we use TICRA Tools [3] for all electromagnetic analyses in this paper.

2 The Hat Feed Optical Design

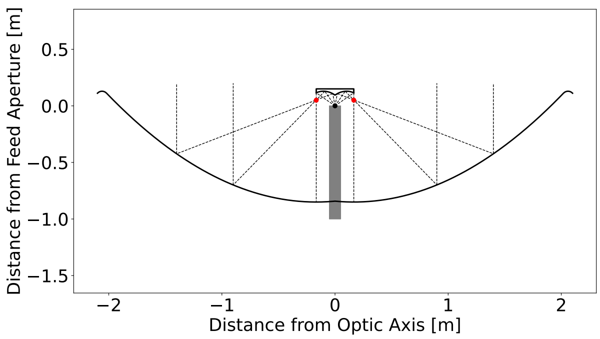

Figure 1. A cross-section of the CGEM starting-point hat feed optical design. The system is a body of revolution. The solid lines represent reflecting surfaces. The grey shaded region denotes the feed column, which contains a feed horn and 1 m of circular waveguide. The dashed lines show typical ray paths.

The Gregorian hat feed system that was the starting point for the CGEM optical design is shown schematically in Figure 1 and is based off of the geometry defined in the TICRA Tools CHAMP3D Ring Focus Wizard [3]. The system is a body of revolution. In the receiving mode, the primary mirror directs signals onto the secondary mirror, which directs them into a feed horn followed by a 1m circular waveguide (shown as the grey region in Figure 1) that carries the signals to our receiver. The primary mirror shape is obtained by offsetting half of a parabola radially from the optic axis and revolving it about the optic axis. The primary mirror thus has a ring focus, which is denoted by the two red dots in Figure 1. The secondary mirror shape is obtained by revolving a section of an ellipse about the optic axis. The geometry of the ellipse is chosen so that one focus overlaps with the focus of the primary and the other focus overlaps with the centre of the feed aperture (black dot in Figure 1). In a geometric optics treatment, plane waves from the sky are thus focused to a ring by the primary mirror and are refocused by the elliptical secondary to the centre of the feed aperture. The secondary mirror will be supported by a radio transparent material (not shown in Figure 1) that will be attached to the outside of the waveguide. Such a ring-focus design can be parameterized with just four parameters: the diameter of the primary (D_p), the diameter of the secondary (D_s), the focal length of the primary (f), and the angle subtended by the secondary when viewed from the centre of the feed (α). As our starting point design, we chose $D_p = 4\,\text{m}$, $f = 1\,\text{m}$, $D_s = 0.3\,\text{m}$, and $\alpha = 60°$. This selection of parameters gives us satisfactory angular resolution for the PGW search ($\sim$0.5°), tolerable aperture blockage, minimal coupling between the feed aperture and stray radiation, and a secondary mirror geometry that is easy to support mecanically. The diameter of the circular waveguide after the feed is 22.82 mm so that the CGEM operating band of 8-10 GHz corresponds to $1.039\, f_{\text{cutoff}} - 1.299\, f_{\text{cutoff}}$. This ensures that the guide only supports the fundamental TE_{11} mode over the operating band while operating as far from cutoff as possible to improve the return loss of the feed. The details of the feed are described in Section 3.2.

3 Optical Design Optimization

3.1 Simulating $T \to P$ Leakage

For the CMB PGW search, we're interested in mapping the sky in Stokes Q and U. Stokes I (referred to as Stokes T in cosmology) on the sky near 9 GHz is expected to be $\sim$1 order of magnitude larger than Stokes Q and U. There are no significant sources of Stokes V in galactic foreground emission and the CMB. Stokes parameters on the sky can be extracted from the auto and cross correlations of orthogonal polarizations measured with an antenna surveying the sky. CGEM will measure polarization in the circular basis so that we obtain Stokes Q and U from cross correlations only, which are uncontaminated by noise bias. If we denote the radiation pattern for port $p \in \{l, r\}$ on the instrument as $\mathbf{A}_p(\hat{\mathbf{n}}) = A_p^{\text{rc}}(\hat{\mathbf{n}})\,\hat{\mathbf{e}}_{\text{rc}} + A_p^{\text{lc}}(\hat{\mathbf{n}})\,\hat{\mathbf{e}}_{\text{lc}}$, then the radiation patterns for an antenna with continuous azimuthal symmetry can be written as

$$\begin{aligned} A_l^{lc} &= \ \ A_{\text{co}}(\theta), & A_l^{rc} &= \ \ A_{\text{cx}}(\theta)e^{2i\phi} \\ A_r^{lc} &= -A_{\text{cx}}(\theta)e^{-2i\phi}, & A_r^{rc} &= -A_{\text{co}}(\theta) \end{aligned} \tag{1}$$

where θ and ϕ are spherical coordinate angles in the telescope frame (with the boresight direction being at $\theta = 0$), and $A_{\text{co}}(\theta)$ and $A_{\text{cx}}(\theta)$ are complex functions that only depend on the angle from boresight and whose functional form is determined by the detailed geometry of the antenna. $|A_{\text{co}}|^2$ is the co-polar beam of the antenna and $|A_{\text{cx}}|^2$ is the cross-polar beam, i.e. the response of port p to the orthogonal polarization q, with $q \neq p$. We've verified with TICRA Tools that our radiation patterns take the form given in Equation 1. With these radiation patterns, the off-diagonal correlation products take the form

$$\begin{aligned} \langle V_r(t)V_l^*(t)\rangle &\equiv W_{rl}(t) \simeq -\tilde{Q}(t) - i\tilde{U}(t) \\ &\quad + \frac{1}{\Omega_{rl}} \int d^2\hat{\mathbf{n}} \left[-2\text{Re}\,(A_{\text{co}}A_{\text{cx}}^*)\, e^{-2i\varphi}\, T(\hat{\mathbf{n}},t) \right] \\ \langle V_l(t)V_r^*(t)\rangle &\equiv W_{lr}(t) \simeq -\tilde{Q}(t) + i\tilde{U}(t) \\ &\quad + \frac{1}{\Omega_{lr}} \int d^2\hat{\mathbf{n}} \left[-2\text{Re}\,(A_{\text{co}}A_{\text{cx}}^*)\, e^{2i\varphi}\, T(\hat{\mathbf{n}},t) \right] \end{aligned} \tag{2}$$

where V_r and V_l denote the signals measured by antenna ports r and l at time t, $\hat{\mathbf{n}}$ denotes the radial unit vector in the telescope coordinate frame, $T(\hat{\mathbf{n}},t)$, denotes the true Stokes T signal, $\Omega_{pq} \equiv \sqrt{\Omega_p\Omega_q}$ is a normalization factor with $\Omega_p = \int d^2\hat{\mathbf{n}}\, |\mathbf{A}_p(\hat{\mathbf{n}})|^2$, and $\tilde{Q}$, $\tilde{U}$ denote the true Stokes parameters on the sky convolved with the azimuthally symmetric main beam $(1/\Omega_{\{rl,lr\}})|A_{\text{co}}|^2$. Here we've assumed that Stokes $V = 0$ and we've dropped terms with integrands $\propto |A_{\text{cx}}|^2\{Q,U\}$ because $T \gg \{Q,U\}$ on the sky near 9 GHz and $2\,\text{Re}\,(A_{\text{co}}A_{\text{cx}}^*) \gg |A_{\text{cx}}|^2$ (verified with TICRA Tools). Notice that, due to the motion of the telescope as it scans the sky, the Stokes terms depend on time in the telescope frame. In the absence of the terms

$$\Delta W_{rl}(t) \equiv \frac{1}{\Omega_{rl}} \int d^2\hat{\mathbf{n}} \left[-2\text{Re}\,(A_{\text{co}}A_{\text{cx}}^*)\, e^{-2i\varphi}\, T(\hat{\mathbf{n}},t) \right] \tag{3}$$

$$\Delta W_{lr}(t) \equiv \frac{1}{\Omega_{lr}} \int d^2\hat{\mathbf{n}} \left[-2\text{Re}\,(A_{\text{co}}A_{\text{cx}}^*)\, e^{2i\varphi}\, T(\hat{\mathbf{n}},t) \right] \tag{4}$$

in Equation 2, we could take linear combinations of W_{rl} and W_{lr} to recover $\tilde{Q}(t)$ and $\tilde{U}(t)$. Equations 3 and 4 describe our most important systematic for measuring polariation, which is the leakage of Stokes T into the off-diagonal correlation products from which we measure Stokes Q and U. We call this $T \to P$ leakage and minimizing this systematic is a central goal in the CGEM optical design. To minimize $T \to P$ leakage, we have to compute Equations 3 and 4 by simulating observations of the sky with CGEM. This is computationally challenging because of the time dependence of $T(\hat{\mathbf{n}},t)$. However, we can evaluate $T \to P$ leakage rapidly by taking the spherical harmonic transform of Equations 3 and 4 and simplifying. The result is

$$\Delta W_{rl}(t) = \sum_{\ell} b_{\ell,2} t_{\ell,2}(t), \quad \Delta W_{lr}(t) = \sum_{\ell} b_{\ell,2} t_{\ell,2}^*(t) \tag{5}$$

where

$$\begin{aligned} b_{\ell,2} &= -\frac{4\pi}{\Omega_{rl}} \sqrt{\frac{2l+1}{4\pi} \frac{(l-2)!}{(l+2)!}} \\ &\quad \times \int_0^{\pi} d\theta \sin\theta\, \text{Re}\,(A_{\text{co}}(\theta)A_{\text{cx}}^*(\theta))\, P_\ell^2(\cos\theta), \end{aligned} \tag{6}$$

$$t_{\ell,2}(t) = \int d^2\hat{\mathbf{n}}\, T(\hat{\mathbf{n}},t) Y_{\ell 2}^*(\hat{\mathbf{n}}). \tag{7}$$

The leakage into Q is given by $\Delta Q(t) = -0.5(\Delta W_{rl}(t) + \Delta W_{lr}(t))$ and the leakage into U is given by $\Delta U(t) = -0.5i(\Delta W_{lr}(t) - \Delta W_{rl}(t))$, respectively. The $T \to P$ leakage can be written as $\Delta P(t) = \sqrt{\Delta Q(t)^2 + \Delta U(t)^2}$, which can be simplified to arrive at

$$\Delta P(t) = |\Delta W_{rl}(t)| = |\Delta W_{lr}(t)|\,. \tag{8}$$

Therefore, an ideal optimization goal is to directly minimize $T \to P$ leakage by minimizing $\Delta P(t) = |\sum_\ell b_{\ell,2} t_{\ell,2}(t)|$. We compute the time-dependent $t_{\ell,2}(t)$ as follows. Given the scan strategy for CGEM and a model for the sky near 9 GHz, we compute the $t_{\ell,2}$ from the model sky in the celestial frame and rotate the $t_{\ell,2}$ at each time-step into the telescope frame using HEALPix [4]. The time resolution is chosen so that every pixel in the HEALPix map that is observed in the CGEM scan strategy is sampled by the telescope boresight. This means that we compute one set of $t_{\ell,2}$ for every pointing needed to observe the Northern sky. This is a highly parallelizable computation that only needs to be done once for a fixed scan strategy and model sky. We use a scaled version of the Haslam 408 MHz map [5] as our model sky. Using the precomputed set of $t_{\ell,2}(t)$, we can easily compute $\Delta P(t) = |\sum_l b_{\ell,2} t_{\ell,2}(t)|$ over the full Northern sky as follows:

- Given an optical design geometry, evaluate the radiation patterns in TICRA Tools to obtain $A_{\text{co}}(\theta), A_{\text{cx}}(\theta)$
- Compute $b_{\ell,2}$ from $A_{\text{co}}, A_{\text{cx}}$ using Equation 6.
- Using the set of precomputed $t_{\ell,2}(t)$ and $b_{\ell,2}$, compute $\Delta P(t) = |\sum_l b_{\ell,2} t_{\ell,2}(t)|$ to get the $T \to P$ leakage at each time (i.e. each telescope pointing).

This allows us to compute our most important polarization systematic in simulated CGEM Northern sky maps for a given optical design in a matter of seconds. We can thus optimize our optical design to minimize $T \to P$ leakage.

3.2 Optimization Procedure

We have three optimization goals: a) maximize the forward gain of our antenna, b) minimize $\Delta P(t)$, and c) minimize the return loss of our antenna. Explicitly, the loss function that we minimize is

$$f = w_G \sum_\nu G_\nu^2 + w_S \sum_\nu S_\nu^2 + w_P \sum_{t,\nu} \Delta P_{t,\nu}. \qquad (9)$$

$G_\nu = \text{Gain}(\nu) - 50\,\text{dBi}$ if $\text{Gain}(\nu) < 50\,\text{dBi}$ and $G_\nu = 0$ otherwise. $S_\nu = \text{Return Loss}(\nu) - (-20\,\text{dB})$ if $\text{Return Loss}(\nu) > -20\,\text{dB}$ and $S_\nu = 0$ otherwise. $\Delta P_{t,\nu}$ is the leakage at each time sample and frequency. w_G, w_S, and w_F are weight factors that are fixed at the start of the optimization so that each of the three goals contributes to the loss an equal amount. We use the hat feed optical design described in Section 2 as the initial optical design in the optimization. The feed we use is a corrugated horn with an asymmetric sine square profile and a variable-depth-slot mode converter, created following the design procedure outlined in [6] for the narrowband case. The primary and secondary mirror surfaces are defined with 10 and 20 evenly spaced points, respectively, which are interpolated with cubic splines. We allow the following parameters (36 in total) to vary in the optical design optimization:

- D_s and α, which are described in Section 2. The ratio f/D_p is held fixed at 0.25 and D_p is fixed to 4 m.
- The 10 nodes defining the primary mirror and the 20 nodes defining secondary mirror. These are only allowed to float in position parallel to the optic axis. The radial positions of the secondary mirror nodes are scaled in proportion to D_s.
- The width-to-pitch ratio of the corrugated horn corrugations, the aperture radius of the corrugated horn, the length of the corrugated horn, and the length ratio of the asymmetric sine-squared profile, as defined in [6].

We use SciPy's L-BFGS-B routine [7] to minimize the loss function in Equation 9. One evaluation of the loss function proceeds as follows:

- Given a set of optical design parameters, call TICRA Tools from Python to evaluate the radiation patterns and return loss for the corresponding optical design.
- Extract the forward gain in dBi from the radiation patterns and evaluate G_ν. Then use the return loss to evaluate S_ν.
- Evaluate $\Delta P_{t,\nu}$ using the procedure described at the end of Section 3.1 at each frequency. Then with all necessary quantities computed, evaluate Equation 9.

It is important to note that this procedure was built incrementally while designing the CGEM optics. This means that the actual design didn't proceed from the starting point design to the optimized design (discussed in the next section) in a single optimization using the above framework. Instead, several preliminary stages of the design were done without a direct leakage computation by instead imposing minimization goals on A_{cx} (which indirectly, and less effectively, reduces the leakage). We also changed the feed multiple times throughout the design process, and in fact the starting point design showcased in the next section used a stepped circular waveguide as a feed rather than a corrugated horn. That said, there is no reason that, with the correct parameterization, the design couldn't have proceeded from the initial design to the optimized design in a single optimization with the above framework. This is how we would have designed the optics in an ideal scenario.

4 Performance

The secondary mirror and feed geometry of the optimized design are shown in Figure 2. The primary mirror is not shown in Figure 2 because the optimized shape only differs from the initial shape by at most 2 cm and is hence hardly noticeable. The small change in the primary mirror shape may be attributable to the fact that the primary mirror was designed before we fully developed the ΔP framework, and so its shape was selected from an optimization with a goal involving A_{cx}. The underlying shape of the secondary mirror deviates significantly from the initial elliptical shape and there are now small-scale ripples in the surface. The parameters defining the corrugated horn hardly changed in the optimization. We note that the forward gain is $\sim$0.25 dB higher across the band and that the return loss is below the goal value of -20 dB at almost all frequencies in the band.

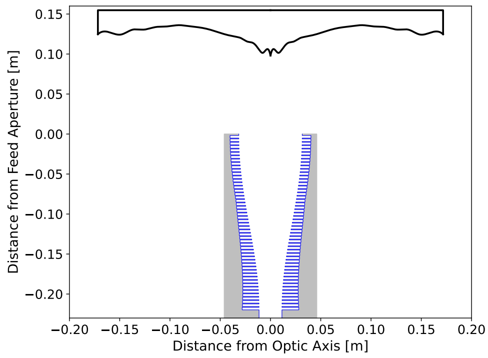

Figure 2. The geometry for the optimized hat feed design, obtained by applying the optimization procedure in Section 3 to the starting point design described in Section 2.

PGWs in the CMB will be detected in spherical harmonic space near ∼100 GHz, and so the most important measure of performance is the angular power spectrum of the ΔP leakage, scaled to 100 GHz. The scaling relation for foreground synchrotron emission is $T_\nu \simeq T_{9\,\mathrm{GHz}}(\nu\,\mathrm{GHz}/9\,\mathrm{GHz})^{-2.7}$ [8]. The angular power spectra of Northern sky ΔP maps, computed through the procedure in Section 3.1 and scaled from the representative frequency of 8 GHz to 100 GHz, for the starting point and optimized designs are shown in Figure 3. The Galactic plane is masked in the power spectrum computation, as is commonly done in a cosmological analysis. The improvement in the leakage power spectrum is ∼2 orders of magnitude or more for scales larger than ∼1° on the sky ($\ell < 180$), which are the most important scales for the PGW search [1].

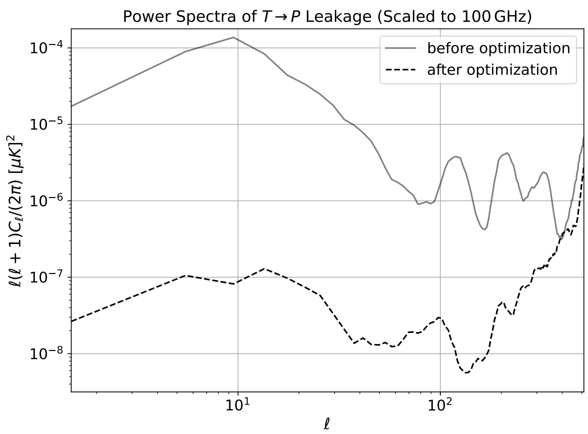

Figure 3. Angular power spectra of simulated 8 GHz Northern sky ΔP maps for the starting point and optimized designs, scaled to 100 GHz. We can see that the leakage power spectrum is greatly reduced for the optimized design, as desired.

5 Conclusion

We have described the CGEM optical design to date and presented an optimization framework that minimizes our most important polarization systematic. The final optimized design greatly outperforms the starting point design in our simulations, with a higher forward gain and an improvement in ΔP leakage (measured in power spectrum space) of several orders of magnitude. The return loss is below the target value of -20 dB over most of the band. We believe that our design demonstrates the power of the hat feed, ring-focus optical design for radio astronomy, and we feel that this design will be useful to other radio astronomers as is, or perhaps even scaled to operate in a different frequency range. We note that we anticipate additional small improvements to the design in the coming months. The optimization procedure that we've outlined here is geared towards CMB foreground measurements. However, the model of our correlation products in Section 3.1 applies to any antenna with continuous azimuthal symmetry, and we believe that the Python/TICRA framework that we've described in Section 3.2 could be adjusted to minimize any systematic that the antenna designer chooses, as long as a reasonable model of the sky can be made. This procedure could thus be particularly useful in other areas of radio astronomy, and perhaps even communications.

Acknowledgements

We would like to thank TICRA and their support team for their helpful insight and numerous useful discussions. We acknowledge the support of the Natural Sciences and Engineering Research Council of Canada (NSERC), [funding reference number 569654].

References

[1] R. L. Workman *et al.*, "Review of Particle Physics," *Prog. Theor. Exp. Phys.*, vol. 2022, p. 083C01, 2022.

[2] P.-S. Kildal, "The hat feed: A dual-mode rear-radiating waveguide antenna having low cross polarization," *IEEE Trans. Antennas Propag.*, vol. 35, no. 9, pp. 1010–1016, 1987.

[3] *TICRA Tools User's Manual*, TICRA, Copenhagen, Denmark, 2022, release 22.0.

[4] K. M. Górski *et al.*, "HEALPix: A Framework for High-Resolution Discretization and Fast Analysis of Data Distributed on the Sphere," *Astrophys. J.*, vol. 622, no. 2, pp. 759–771, Apr. 2005.

[5] M. Remazeilles *et al.*, "An improved source-subtracted and destriped 408-MHz all-sky map," *Mon. Not. R. Astron. Soc.*, vol. 451, no. 4, pp. 4311–4327, Aug. 2015.

[6] C. Granet and G. James, "Design of corrugated horns: a primer," *IEEE Trans. Antennas Propag.*, vol. 47, no. 2, pp. 76–84, 2005.

[7] P. Virtanen *et al.*, "SciPy 1.0: Fundamental Algorithms for Scientific Computing in Python," *Nat. Methods*, vol. 17, pp. 261–272, 2020.

[8] P. Platania *et al.*, "Full sky study of diffuse Galactic emission at decimeter wavelengths," *Astron. Astrophys.*, vol. 410, pp. 847–863, Nov. 2003.